

NPA/Int. 69-5
9.5.69

27/09/2013

Chlorophyll a fluorescence

MAGNETIC FIELD

Journal of Clinical Anesthesia 1999; 13: 100-106

Wetlands are ecosystems that are characterized by water-saturated soil conditions, which support unique plant and animal communities.

MAGNETIC FIELD DISTRIBUTION MEASUREMENTS IN THE GARGAMELLE

BUBBLE CHAMBER MAGNET

POLY(1-PHENYL-1-PROPYNE)

the life of a man by the time he reaches middle age.

R. Grüb and J.M. Mauqain

卷之三

1960-61
1961-62

198. *Leptodora histrio* (L.) Schleicher, 1853. *Leptodora histrio* Linné, 1758.

卷之三十一

1996-1997-1998

PS/7196

CONTENTS

- I) INTRODUCTION
- II) GENERAL DESCRIPTION
 - II.1) Magnetic Measurement Method
 - II.2) Mechanical Support
 - II.3) Recording of Measurements
- III) MECHANICS
- IV) ELECTRONICS
 - IV.1) Hall Plate Equipment Electronics
 - IV.2) Data Acquisition Electronics
- V) DATA REDUCTION
- VI) RESULTS
- VII) ACCURACY OF THE MEASUREMENTS
- VIII) MODIFICATIONS FOR FINAL MEASUREMENTS
- IX) ACKNOWLEDGEMENTS
- X) REFERENCES

FIGURE CAPTIONS

Figure 1 : Block diagram of set-up

Figure 2 : Mechanical support (schematic)

Figure 3 : Reference frame

Figure 4 a: Picture of mechanical support

Figure 4 b: Picture of probe holder

Figure 5 : Picture of control and display racks

Figure 6 : Computer print-out

Figure 7 : Magnetisation curve

Figure 8 : BX along X axis

Figure 9 : BY along X axis

Figure 10 : BZ along X axis

Figure 11 : BZ along circle $R_o = 85 \text{ cm}$, $X_o = 120 \text{ cm}$ at $I = 9000 \text{ A}$

Figures 12 - 23 12 typical plots of BZ made by the Calcomp plotter

$I = 9000 \text{ A.}$

I) INTRODUCTION

The magnetic field distribution of the Gargamelle bubble chamber magnet has been measured (without the chamber body) as an engineering and manufacturing quality test. For this purpose a few thousand points in the downstream half of the magnet need to be measured. These measurements also permitted the testing and commissioning of the whole measuring and recording equipment and the data reduction instrumentation. This experience enabled us to decide on necessary or useful modifications for the final measurements to be performed later with the chamber body mounted into the magnet.

II) GENERAL DESCRIPTION

The aim is to measure 11000 points throughout the 10 m^3 chamber with a good accuracy in position and flux density but also without any fixation inside the magnet and with little space available. between the magnet coils to introduce the measuring probe. With the great number of points to be measured and the relatively short time available (a few days), a certain degree of automation was required.

To avoid making the system too complicated and expensive, we have chosen the following measurement method and set up.

I.1 Magnetic Measurement Method

The three components BX, BY, BZ are measured independently using three Hall probes for the X, Y, Z plane respectively.

Initially the BX field plot is made, then the BX probe is replaced by the BY probe and the BY field plot made similarly for BZ. The reason for this procedure is that it was thought important to measure the three components exactly at the same points in space.

Each Hall plate has its own Hall generator.

A fixed Hall plate sensitive to the main component BZ gives a flux density BI which must be a constant signal all through the measurements and which permits, if necessary, to apply during computation a correction to the X, Y, Z Hall voltages, to adjust them to the nominal magnet current for which the mapping is being made.

All the probes are thermally stabilized by a heating element controlled by a thermistor. A second temperature calibrated thermistor inside the probe gives a direct checking and reading of the temperature.

I.2 Mechanical Support

The reference frame attached to the magnet is shown in Fig. 3. The support has been designed according to the principle shown in Fig. 2. The probe describes a circle around the X axis taking precise angular positions Θ with possible increases of 7.5° , 15° or 30° .

Having described a circle, the longitudinal X_o position is varied manually to a new point, minimum increase of 10.0 cm, so it is possible to describe a whole cylinder around the X axis.

Then one displaces manually the radial position of the probe R_o (increase 9.75 cm). This is the only case where one needs to enter the chamber. The R_o , X_o , T_o positions are precisely reproducible since all are mechanically locked. The mechanical assembly is made to measure one half of the chamber (along X axis).

I.3 Recording of Measurements

As soon as the probe is locked in a position, the Hall voltages (probe and reference) and the position voltages (X_o , T_o , R_o) obtained with potentiometers for X_o , T_o and with a chain of resistances for R_o) are measured by a digital voltmeter and simultaneously printed out and punched out on a paper tape according to Fig. 1.

III) MECHANICS

Fig. 5 shows a picture of the mechanical support. Ref. 1 reports in detail about the mechanical design and construction. The particular solution here is that the probe constitutes a pendulum because one wanted to record directly the BX, BY, BZ components and not the BX, BR, BT components.

The Hall probe positions are locked with a precision of ± 0.5 mm (taking into account all the alignment and mechanical errors).

IV) ELECTRONICS

IV.1 Hall Plate Equipment Electronics

The Hall plates selected for the measurements are the FC 33 Siemens type having a low temperature coefficient.

The 100 mA constant Hall current is given by the Siemens K 11 supply with a stability of $\pm 5 \cdot 10^{-4}$. The Hall plate is located next to two thermistors in a copper bar around which is wound a heating wire coil. The whole is contained in a box having a good thermal insulation.

The temperature regulation (ref. 2) controlled by one thermistor and which can be checked with the second one ($10 \text{ mV}/^\circ\text{C}$) is $\pm 0.2^\circ\text{C}$. The temperature error of the Hall constant RH is

$$\frac{\Delta \text{RH}}{\text{RH}} = \frac{\Delta \beta}{\beta} \cdot \Delta t$$

β being the temperature coefficient for the open circuit Hall voltage. We do not take into account the temperature coefficient for the Hall voltage circuit inner resistance since the load has a very high resistance (digital voltmeter).

$$\beta = 0.04 \% /^\circ\text{C}$$

$$\frac{\Delta \text{RH}}{\text{RH}} \simeq 10^{-4}$$

A switching unit permits selection and read out on a digital voltmeter H.P. 5254 L + 5265 A of the Hall current and the temperature for the measuring and reference probes.

IV.2 Data Acquisition Electronics

The NPA Electronic Workshop has designed and constructed (ref. 3) a special Data Acquisition and Measuring Equipment (D.A.M.E.) The D.A.M.E. system scans the input information routing each in turn to an integrating digital voltmeter D.M. 2022 which sends by means of a buffer memory and under control of a Control Unit the outputs sequentially to the Print and Punch Units (Fig. 1 and 5)

with the required format programming facilities. Ref. 4 reports in detail about the D.A.M.E. system. In the present case, as soon as the probe is locked in a position, the following information are automatically punched on the paper tape in BCD 8421 characters.

(\pm) V1V2V3V4	(\pm) I1I2I3I4	(\pm) R1R2	(\pm) X1X2	(\pm) T1T2
Hall voltage of measuring probe in 0.1 mV	Hall voltage of reference probe in 0.1 mV	Radial position in mV	Axial position in mV	Angular position in mV

V) DATA REDUCTION

The paper tape is punched in BCD 8421 characters and is converted to external BCD information on a half-inch magnetic tape via the IBM 1401 using the standard BCD conversion program 3.25.

Those characters can then be read directly by the 6000 series computers in an A format.

A program has been developed which, after checking, converts each A format character in an I format character enabling then computation. It calculates the flux density from the Hall voltages by reading the calibration curves of the Hall plates. The measured points of the calibration curve have been interpolated by a 6th order polynomial least squares fit (library program F 202).

The field map is then printed in a suitable form (Fig. 6) and field plots are obtained by off-line plotting (library program J 502).

VI) RESULTS

Some typical plots of BZ are given in Fig. 12 - 23. A computer output including all the measurements performed on the Gargamelle magnet (without chamber body) is available in the NPA/PBT Group.

VII) ACCURACY OF THE MEASUREMENTS

The Hall plates have been calibrated with a nuclear resonance flux-meter.

We summarize here all the errors of the measurement.
(relative errors when possible and absolute errors in the other cases).
PS/7196

- position error of Hall plate centre ± 0.5 mm in all directions
- calibration error $\pm 10^{-4}$ Tesla
- interpolation error of calibration curve $\pm 5 \cdot 10^{-5}$
- error due to Hall current instability $\pm 5 \cdot 10^{-4}$
- error due to variation of RH (Hall constant) with temperature $\pm 10^{-4}$
- error due to angular position uncertainty of Hall plate : for BX : ± 0.0075 Tesla (± 5 mr around Y)
: for BY ± 0.0230 Tesla (± 14 mr around X)
: for BZ $\pm 10^{-4}$ (± 14 mr around X)

This error is a systematic one along a generating line.

The measurement of the main component BZ comes out to have the following accuracy :

$$\frac{\sum \Delta BZ}{BZ} \simeq 10^{-3}$$

(without taking into account the ± 0.5 mm uncertainty on the position of the Hall plate centre).

The measurement of the components BX and BY is unprecise (relatively speaking) since those are very small but

$$\frac{\sum BX}{BZ} = 5 \text{ o/oo}$$

$$\frac{\sum BY}{BZ} = 1.5 \%$$

VIII) MODIFICATIONS FOR FINAL MEASUREMENTS

To speed up the measurements, the 3 components will be measured at once so reducing the total measurement time by 3.

A probe holder containing the X, Y, Z Hall plates fed in series will be designed. Those will be located on an axis parallel to the X axis, the centres being 15 mm apart. One will try also to minimize the errors on BY and BX due to the angular position uncertainty of the Hall plates.

IX) ACKNOWLEDGEMENTS

We thank J.C. Gallay who designed and constructed the mechanical support, N. Cajano and P. Actis who developed the data acquisition and measuring equipment (D.A.M.E.), and Mr. van Gulik who kindly made available to us the necessary calibration facilities. Acknowledgement are also due to Mr. Ohayon for useful discussions and information concerning the magnet and to B. Langeseth.

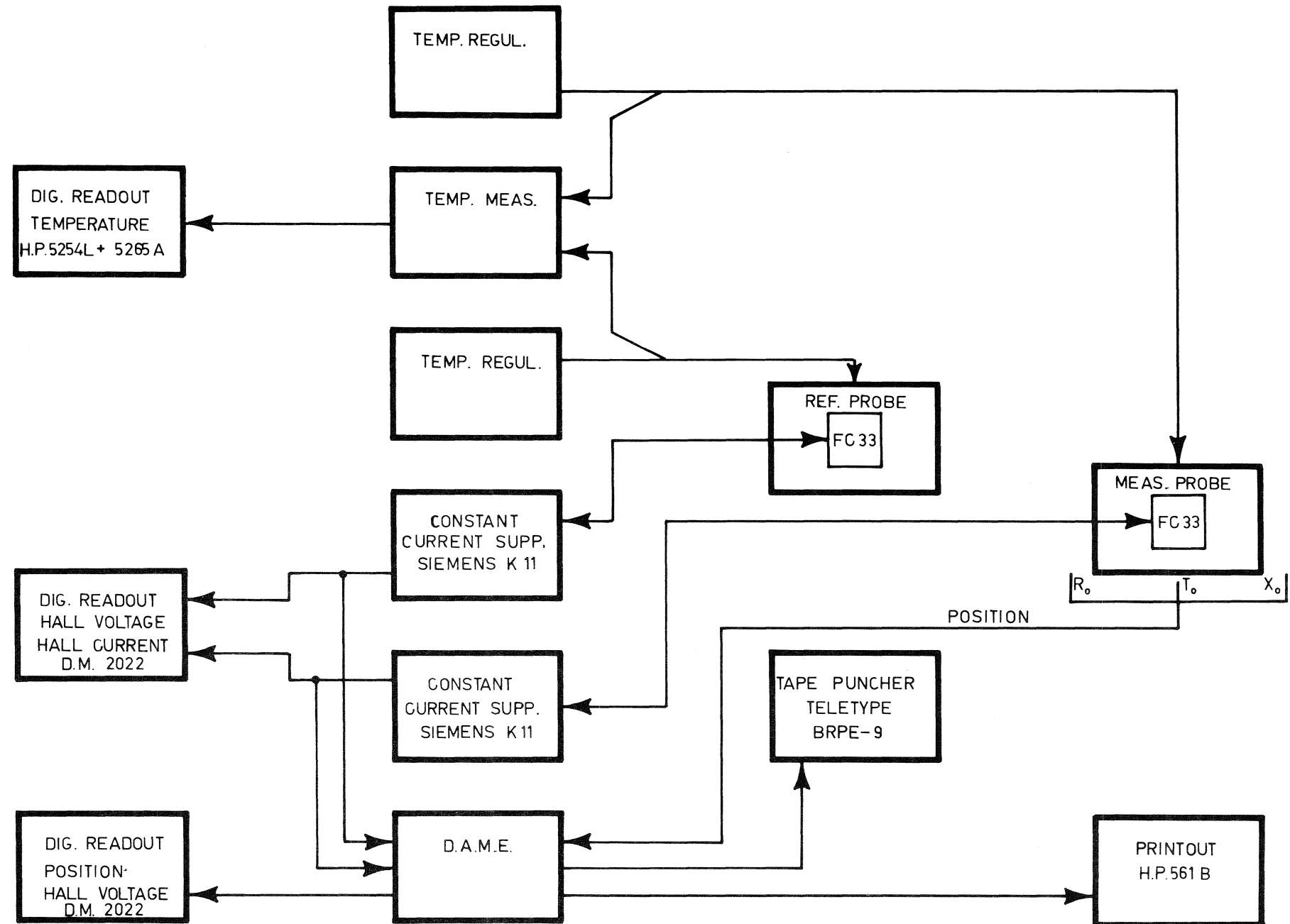
We are grateful to Dr. C.A. Ramm who supported this work.

Distribution : (open)

Scientific staff of N.P.A. Division

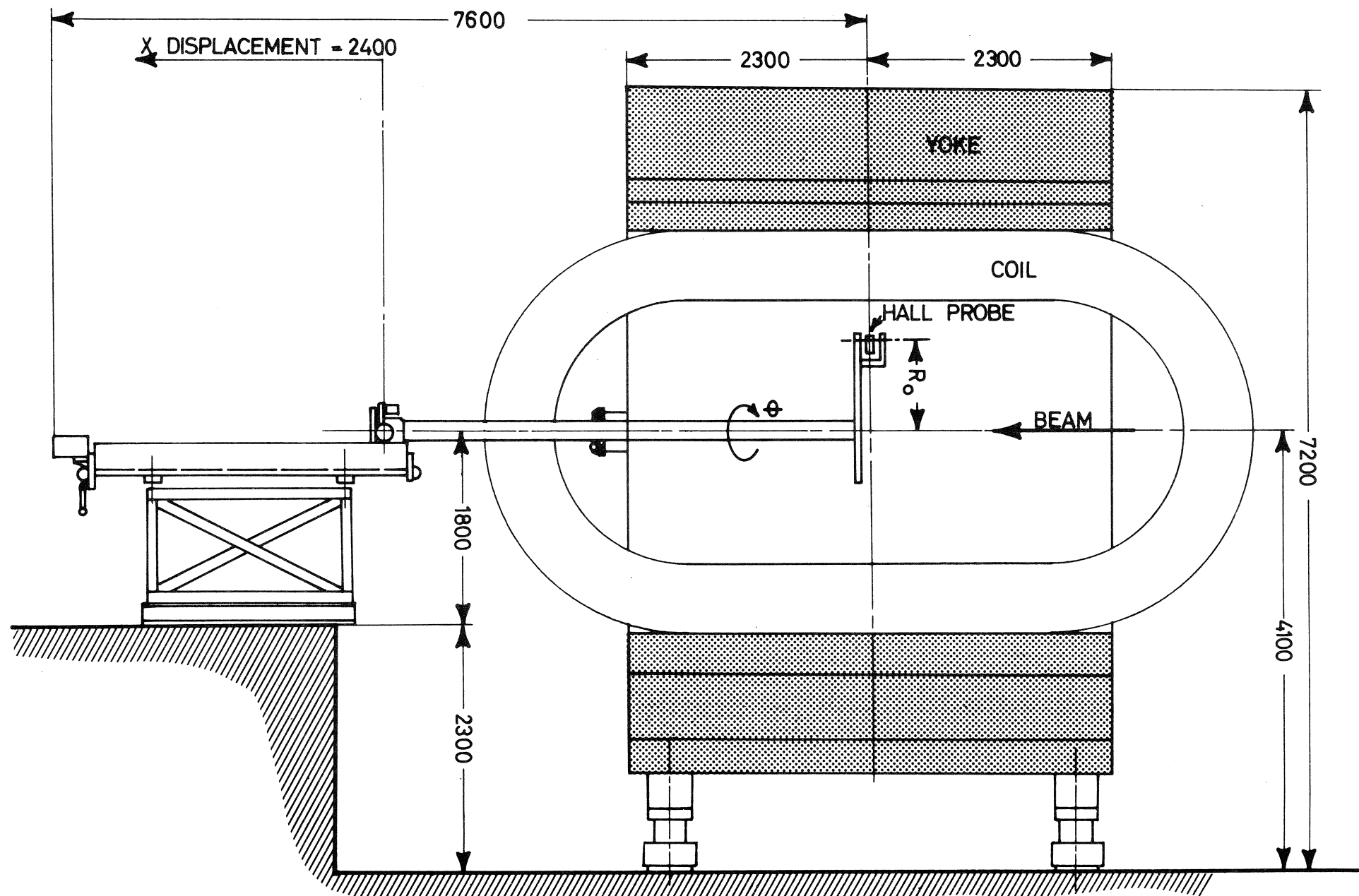
REFERENCES

1. J.C. Gallay - Partie mécanique du dispositif de mesure magnétique de l'aimant Gargamelle.
2. P. Actis - Report (to be published)
3. N. Cajano, G. Kuhn - Data acquisition and measuring equipment D.A.M. E., preliminary specifications.
4. P. Actis, N. Cajano - report in preparation.



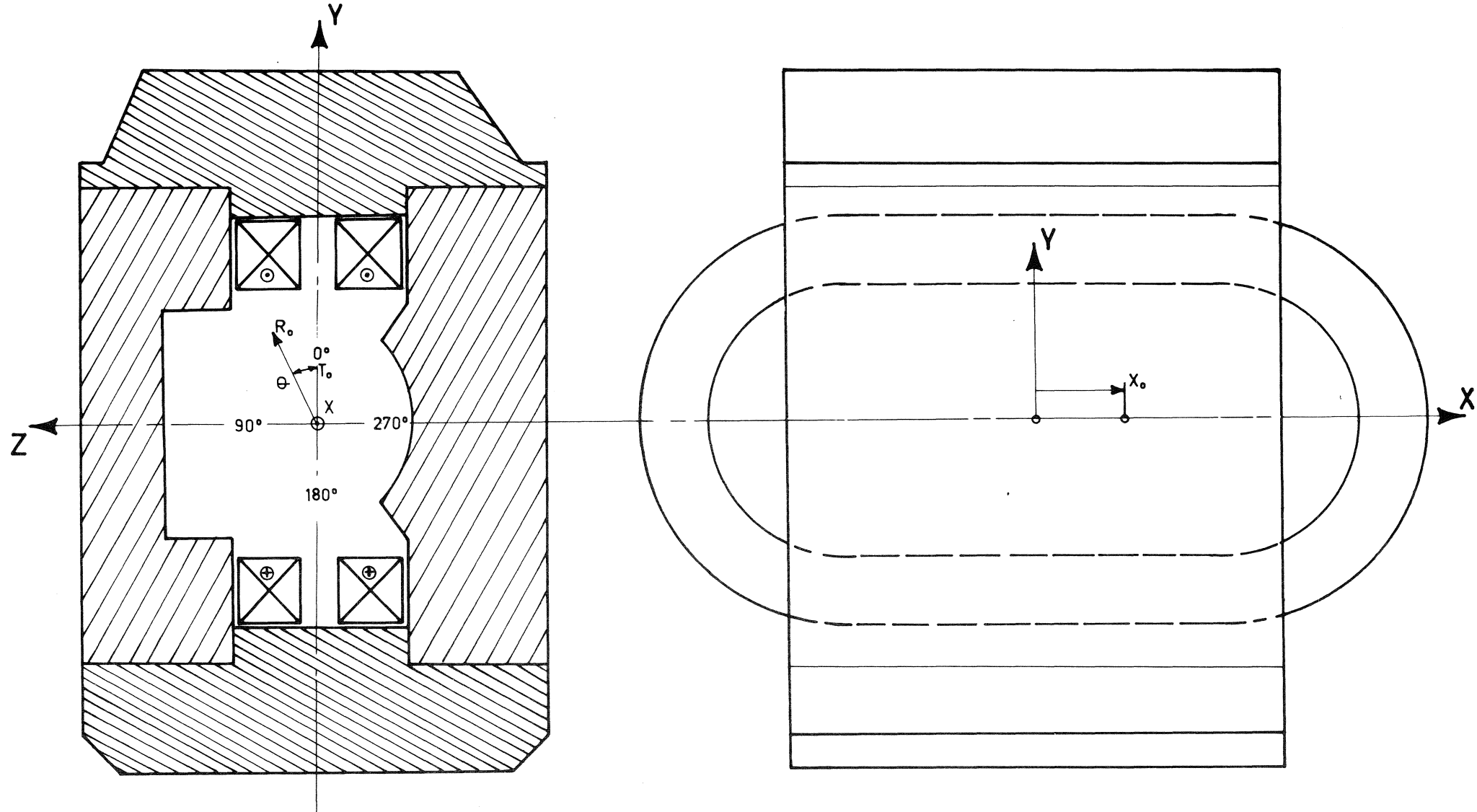
BLOCK DIAGRAM

FIG.1



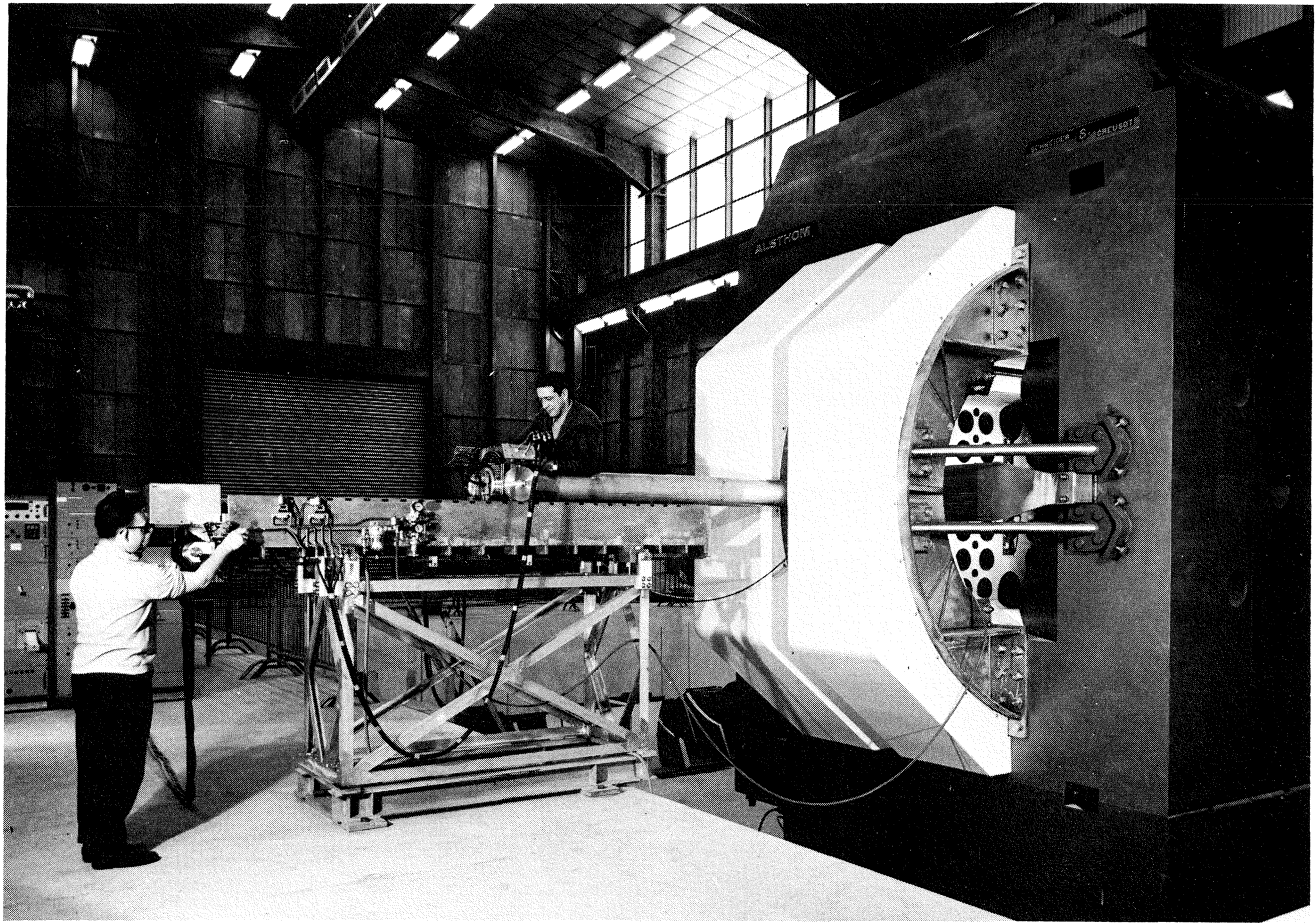
MECHANICAL SUPPORT

FIG.2



REFERENCE FRAME

FIG. 3

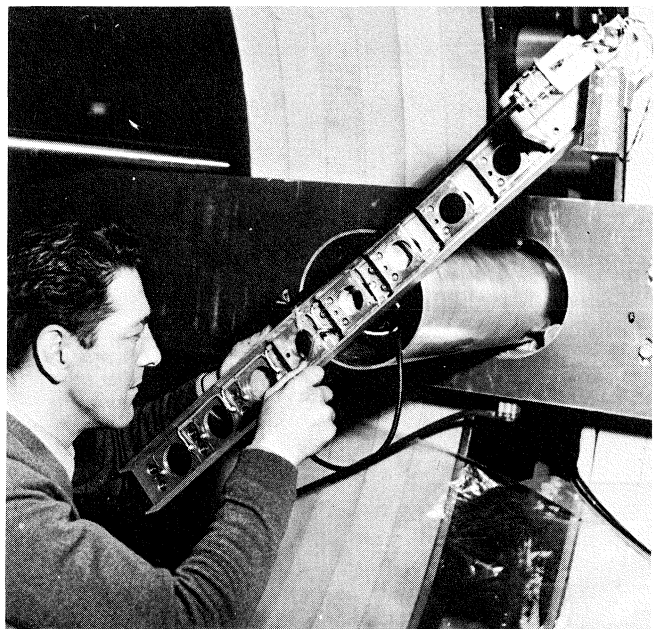


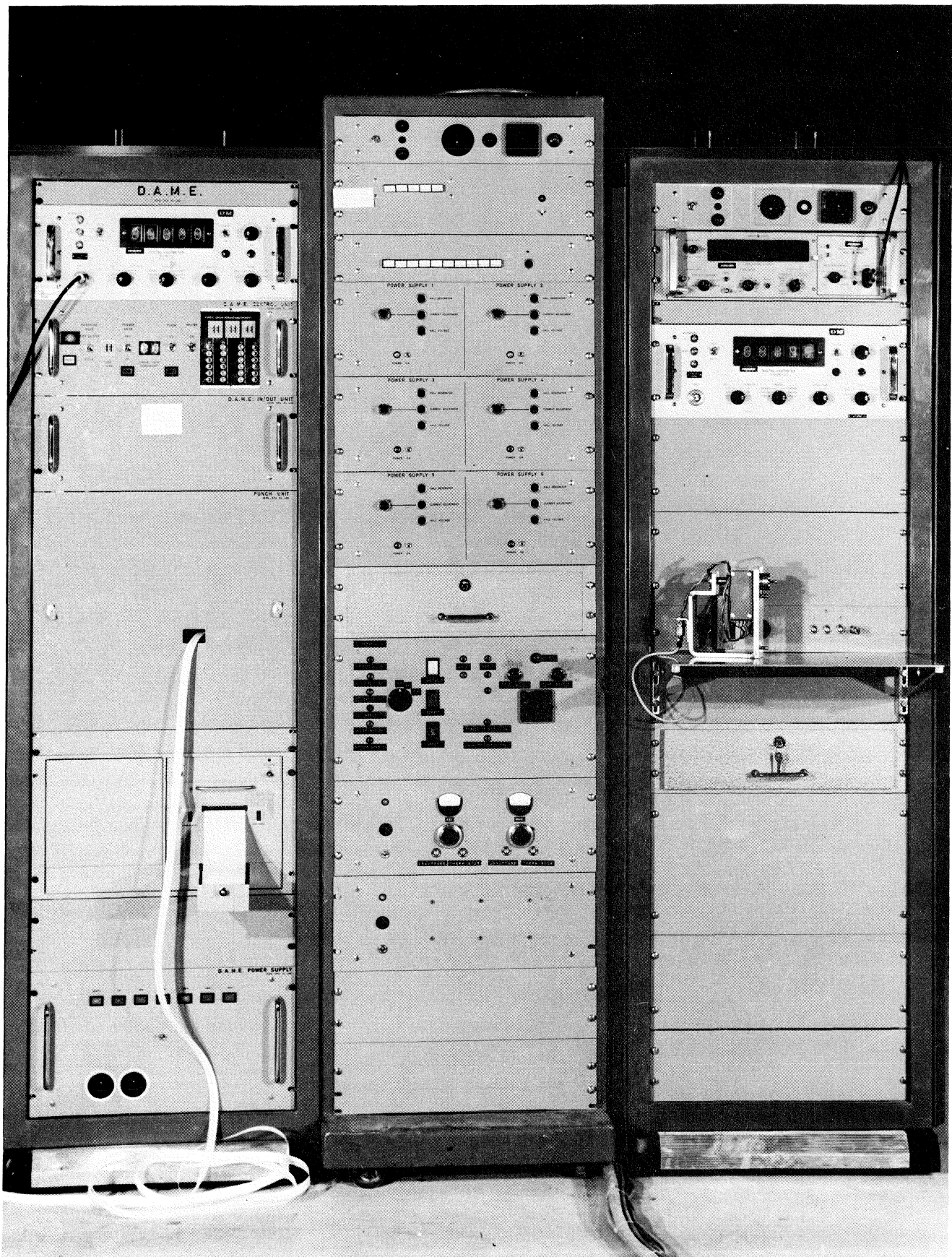
VIEW OF MEASURING DEVICE

FIG. 4a

VIEW OF PROBE HOLDER

FIG. 4b

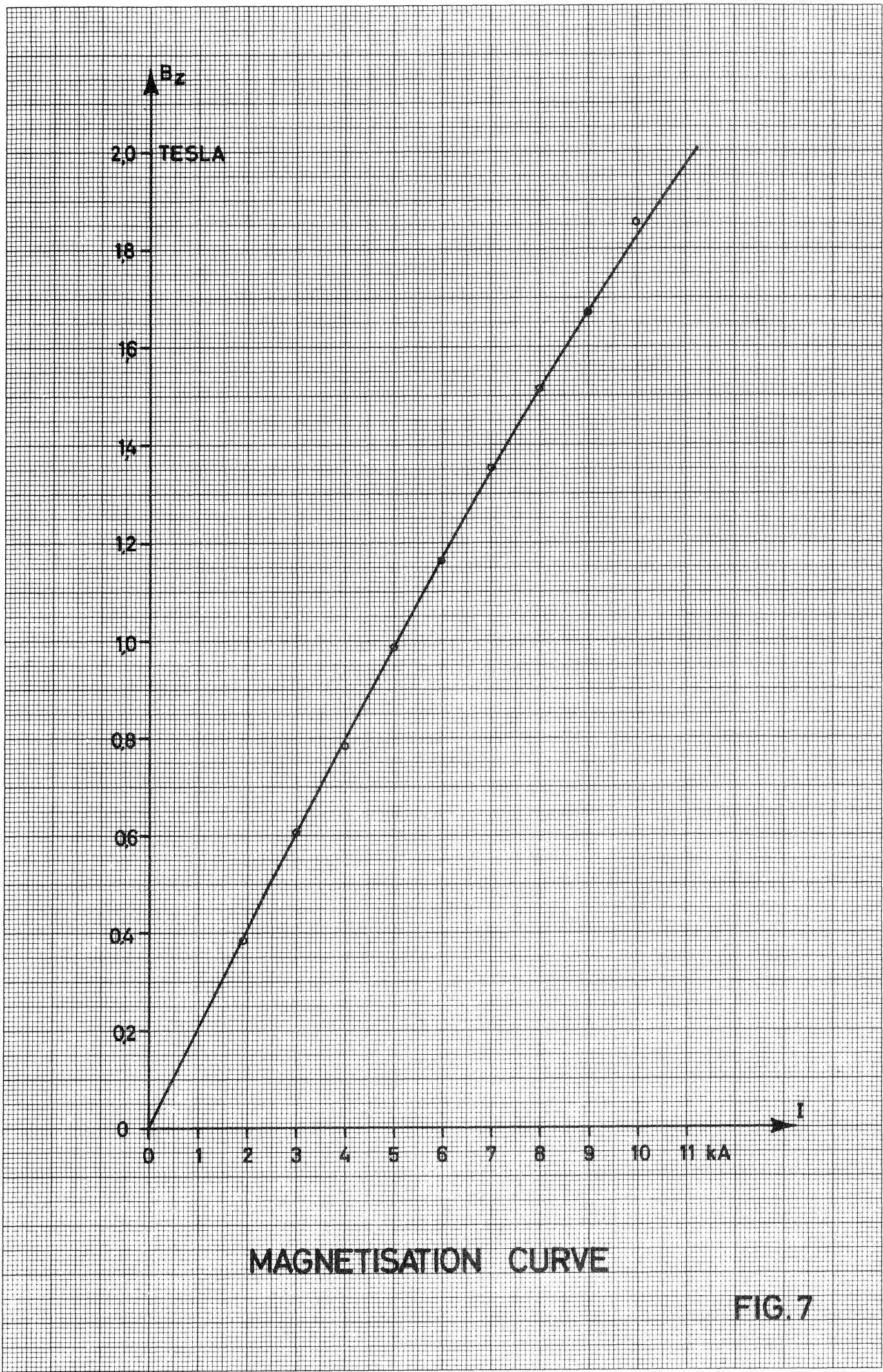


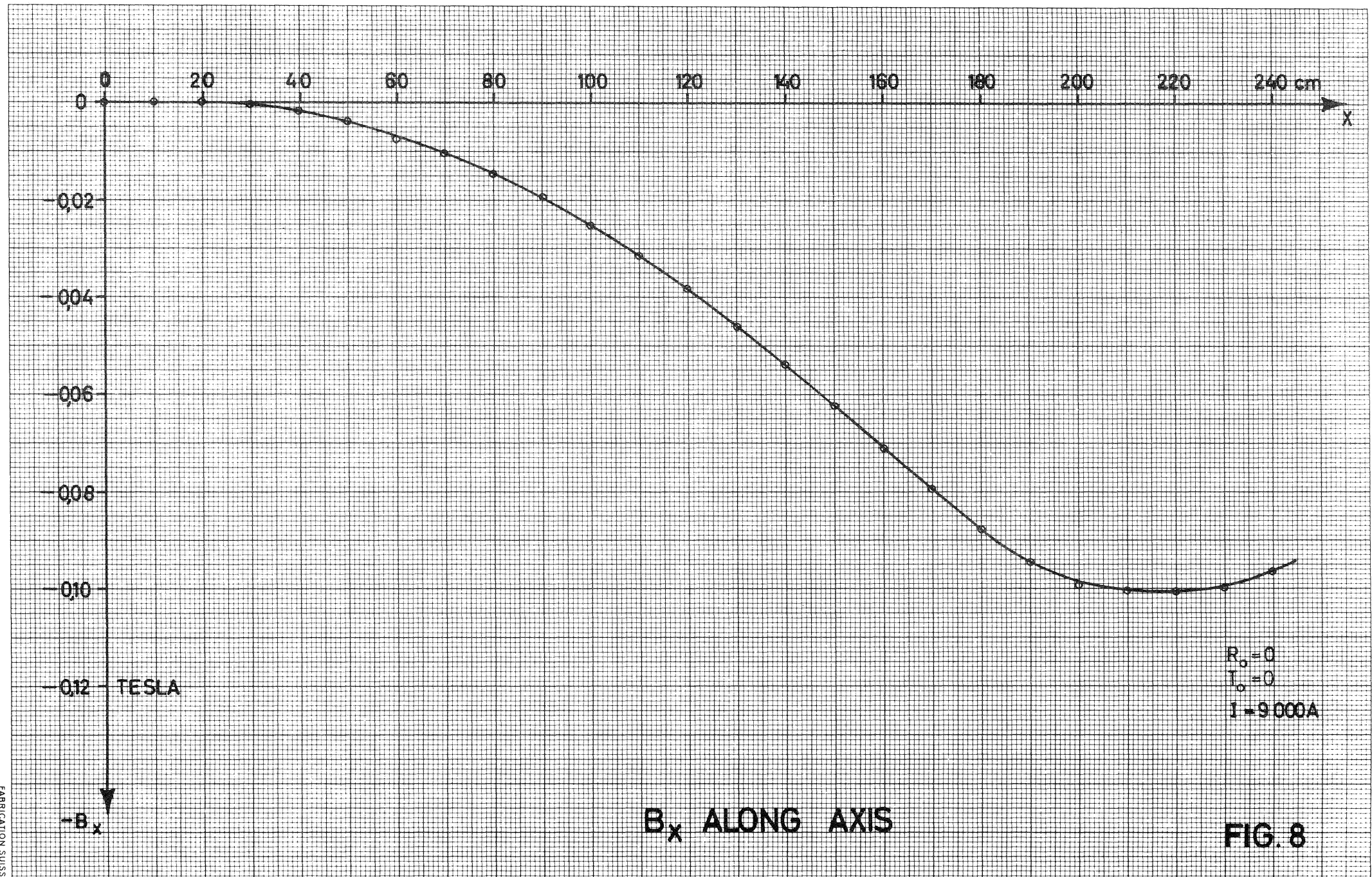


VIEW OF CONTROL AND DISPLAY RACKS

FIG. 5

K1	I1	J1		R0	X0	T0	BZ	BI	BZC
RADIAL	AXIAL	TETA		RADIAL (CM)	AXIAL (CM)	TETA (DEGREE)	RZ (TESLA)	BI (TESLA)	BZC (TESLA)
6	6	0	*	57.00	60.00	0.00	-1.7717	-1.2943	-1.7710
6	6	1	*	57.00	60.00	7.50	0.0000	0.0000	I
5	6	2	*	57.00	60.00	15.00	-1.7292	-1.2943	-1.7285
6	6	3	*	57.00	60.00	22.50	0.0000	0.0000	I
5	5	4	*	57.00	60.00	30.00	-1.6708	-1.2943	-1.6701
5	5	5	*	57.00	60.00	37.50	0.0000	0.0000	I
5	5	6	*	57.00	60.00	45.00	-1.5977	-1.2943	-1.5971
5	5	7	*	57.00	60.00	52.50	0.0000	0.0000	I
5	5	8	*	57.00	60.00	60.00	-1.5333	-1.2943	-1.5327
5	6	9	*	57.00	60.00	67.50	0.0000	0.0000	I
5	6	10	*	57.00	60.00	75.00	-1.4944	-1.2943	-1.4938
5	5	11	*	57.00	60.00	82.50	0.0000	0.0000	I
5	5	12	*	57.00	60.00	90.00	-1.4836	-1.2943	-1.4830
5	5	13	*	57.00	60.00	97.50	0.0000	0.0000	I
5	5	14	*	57.00	60.00	105.00	-1.4968	-1.2943	-1.4962
5	5	15	*	57.00	60.00	112.50	0.0000	0.0000	I
5	6	16	*	57.00	60.00	120.00	-1.5375	-1.2943	-1.5369
5	6	17	*	57.00	60.00	127.50	0.0000	0.0000	I
5	5	18	*	57.00	60.00	135.00	-1.6038	-1.2943	-1.6031
5	5	19	*	57.00	60.00	142.50	0.0000	0.0000	I
5	6	20	*	57.00	60.00	150.00	-1.6763	-1.2943	-1.6763
5	6	21	*	57.00	60.00	157.50	0.0000	0.0000	I
5	5	22	*	57.00	60.00	165.00	-1.7338	-1.2943	-1.7331
5	5	23	*	57.00	60.00	172.50	0.0000	0.0000	I
5	6	24	*	57.00	60.00	180.00	-1.7763	-1.2943	-1.7756
5	6	25	*	57.00	60.00	187.50	0.0000	0.0000	I
5	5	26	*	57.00	60.00	195.00	-1.8091	-1.2943	-1.8084
5	5	27	*	57.00	60.00	202.50	0.0000	0.0000	I
5	5	28	*	57.00	60.00	210.00	-1.8151	-1.2943	-1.8151
5	5	29	*	57.00	60.00	217.50	0.0000	0.0000	I
5	6	30	*	57.00	60.00	225.00	-1.7625	-1.2943	-1.7618
5	5	31	*	57.00	60.00	232.50	0.0000	0.0000	I
5	5	32	*	57.00	60.00	240.00	-1.6726	-1.2943	-1.6726
5	5	33	*	57.00	60.00	247.50	0.0000	0.0000	I





0 20 40 60 80 100 120 140 160 180 200 220 240 cm

X

0.2

-0.4

-0.6

-0.8

-1.0

-12×10^{-2} TESLA

B_y

B_y ALONG AXIS

$R_o = 0$
 $T_o = 0$
 $I = 9000A$

FIG. 9

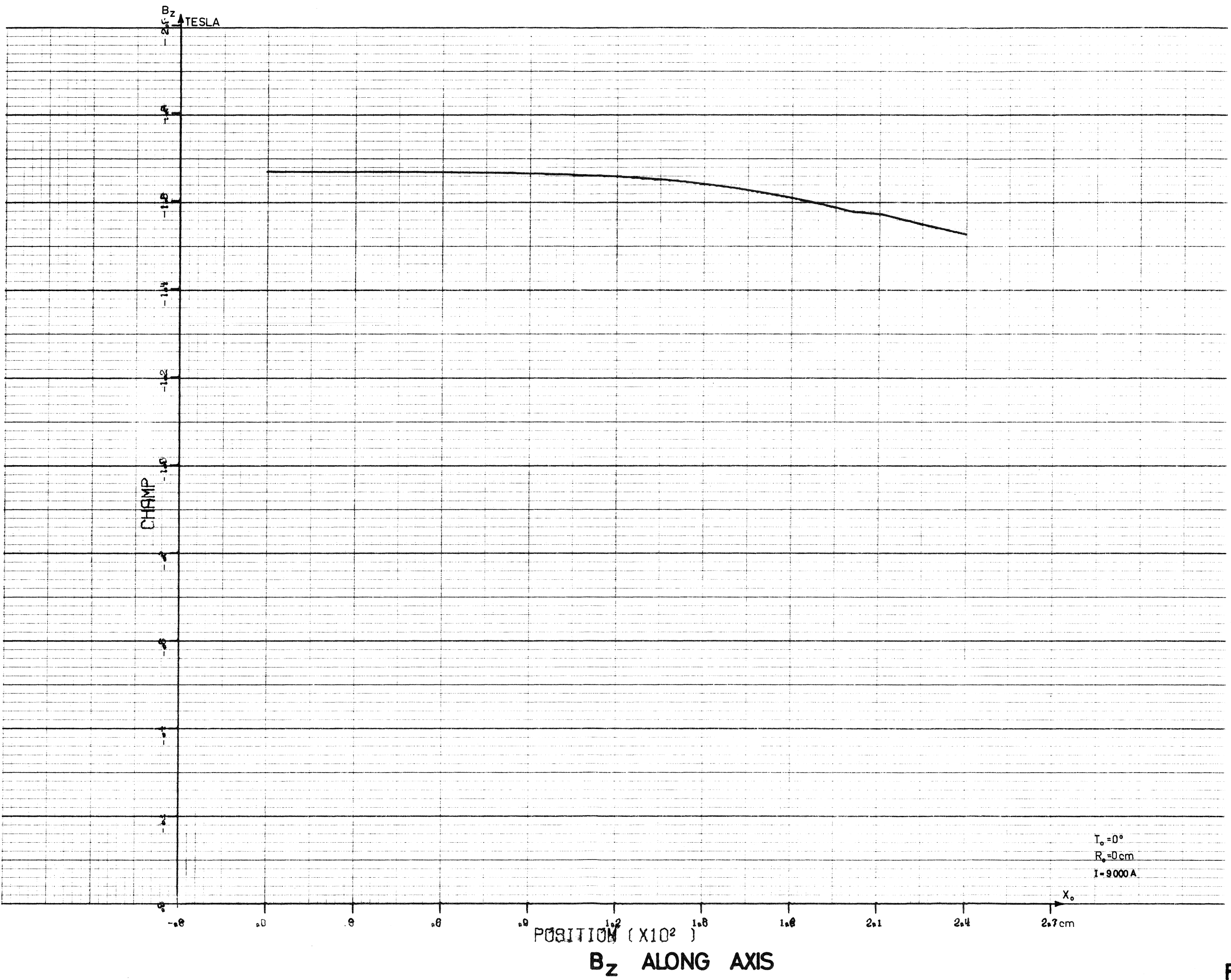
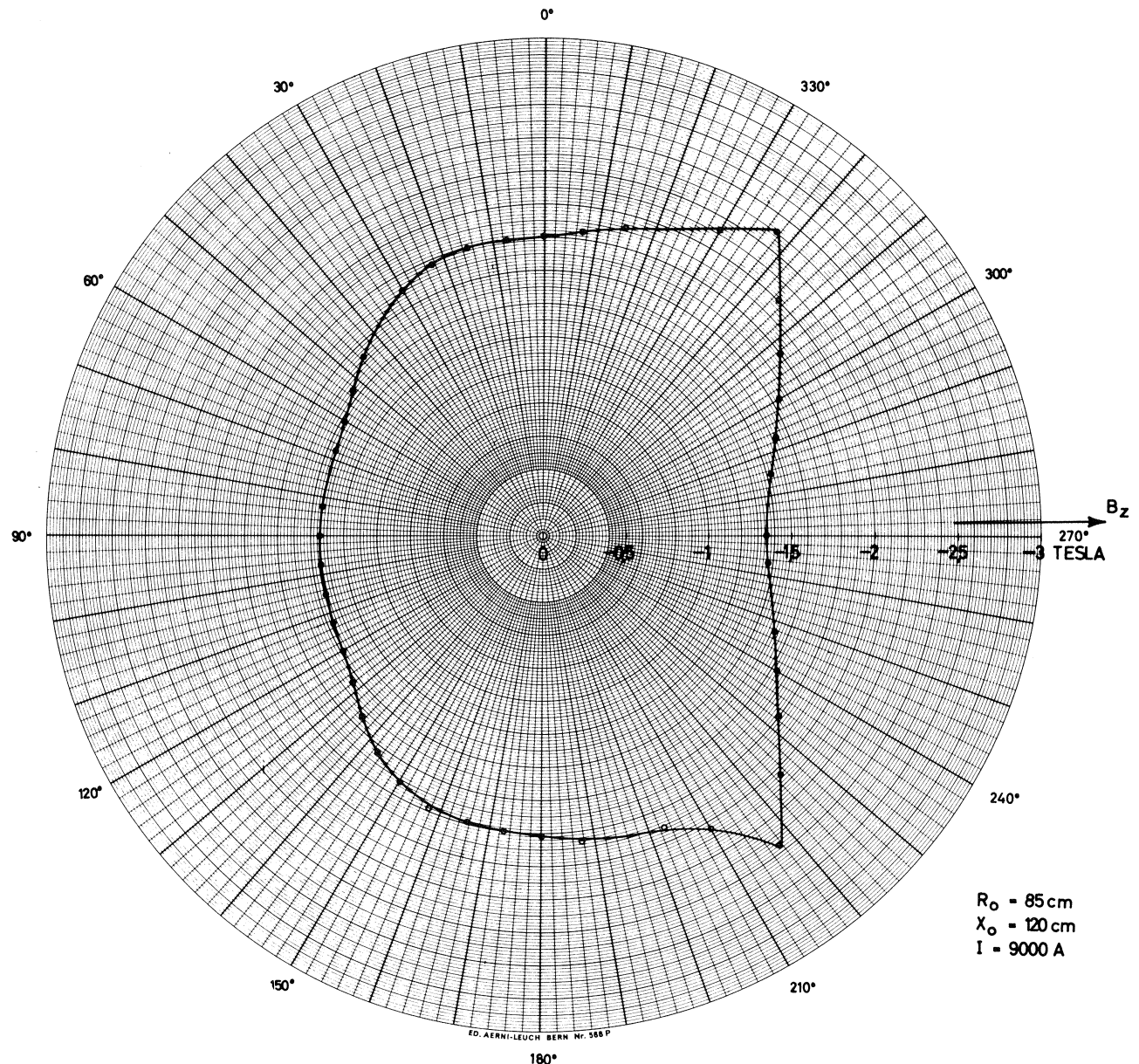


FIG. 10



B_z ALONG CIRCLE

FIG. 11

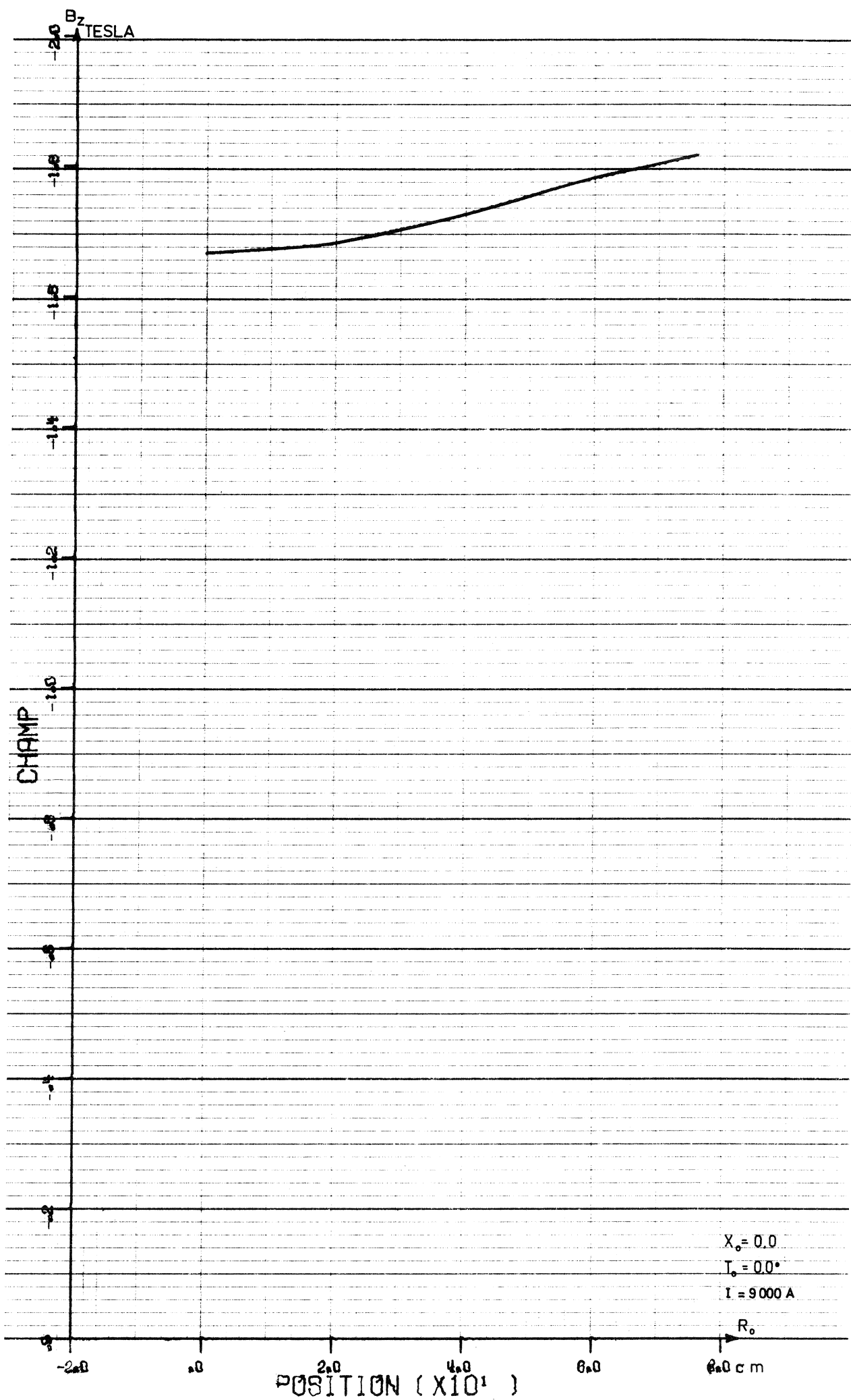


FIG. 12

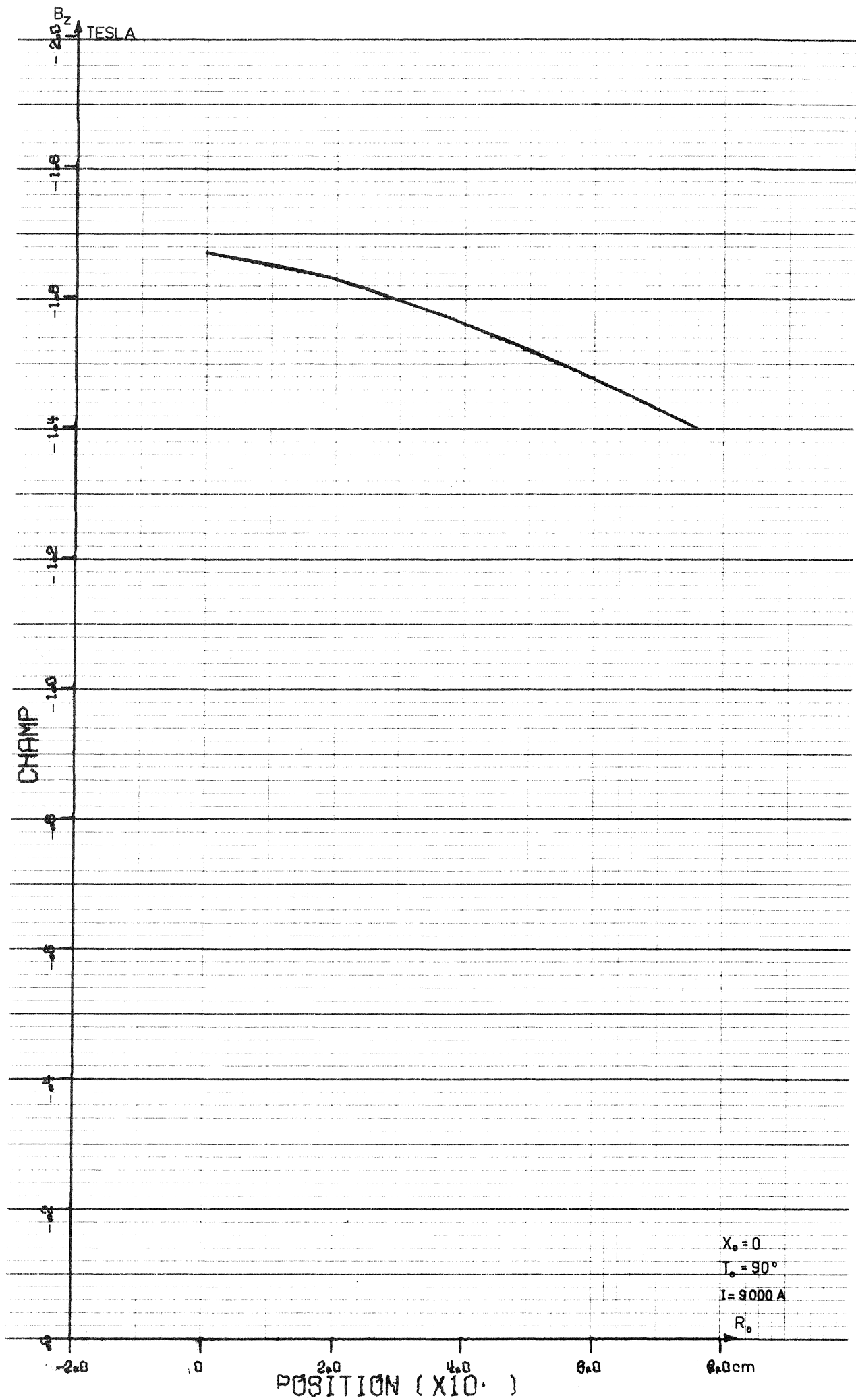


FIG.13

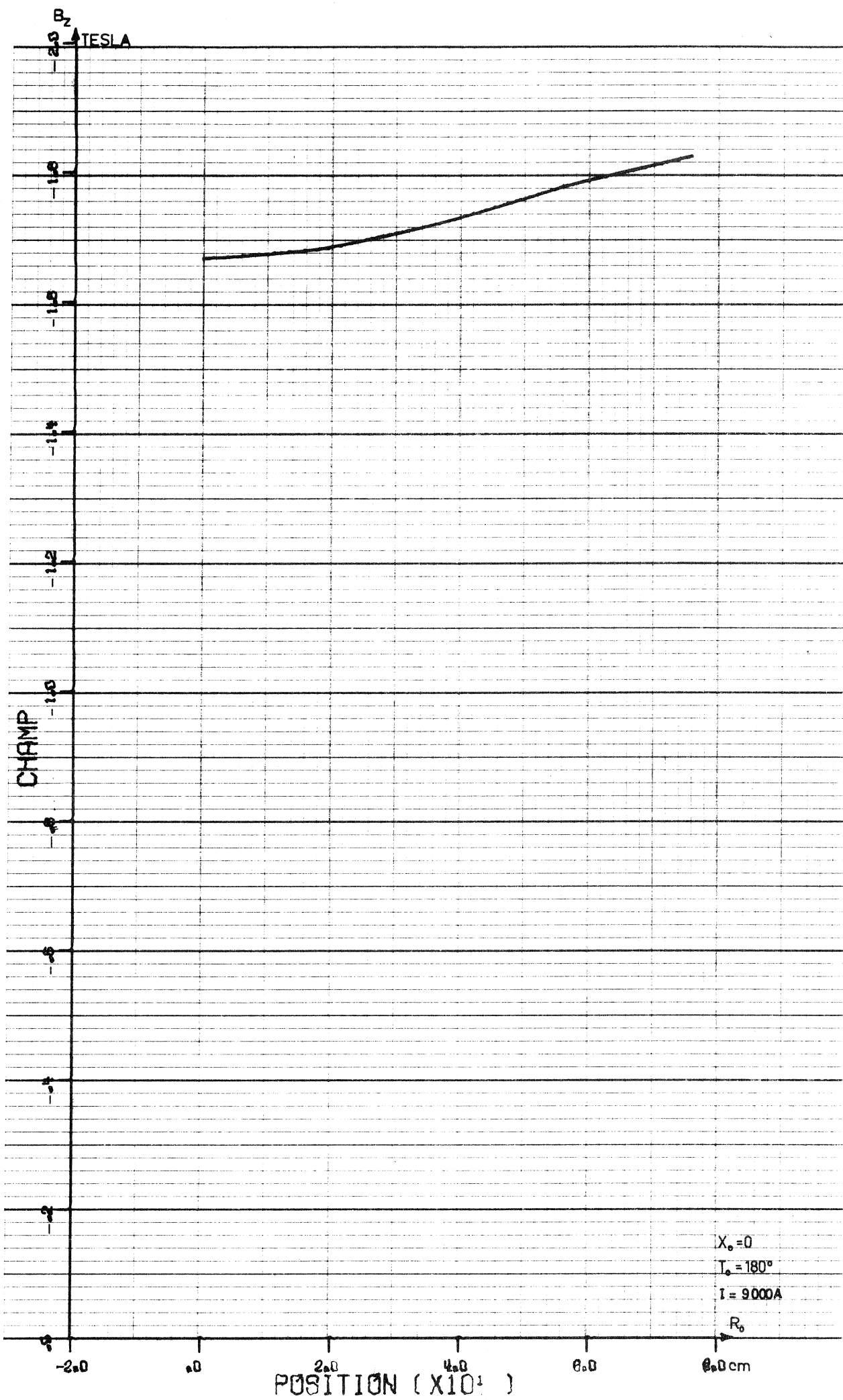


FIG. 14

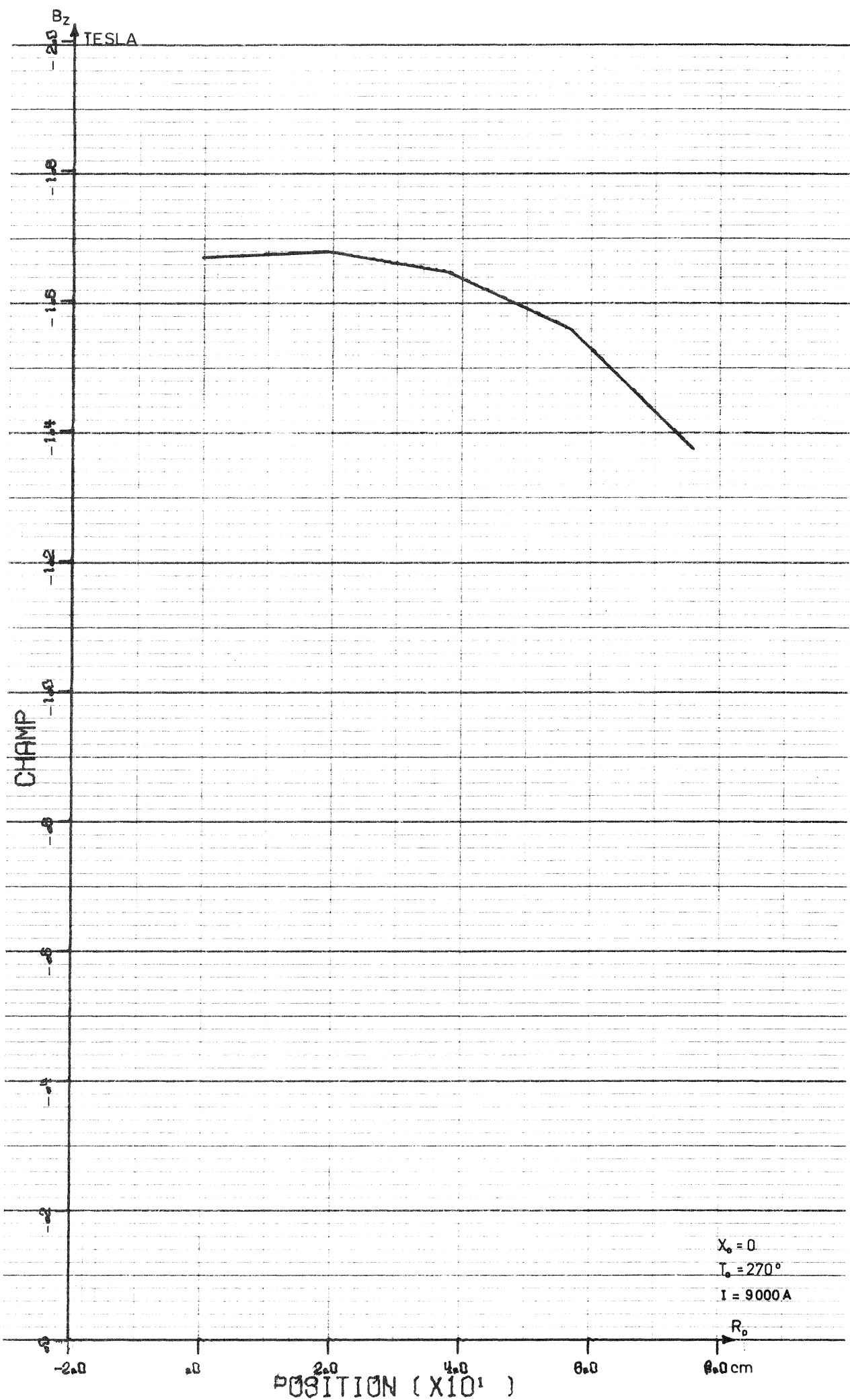


FIG. 15

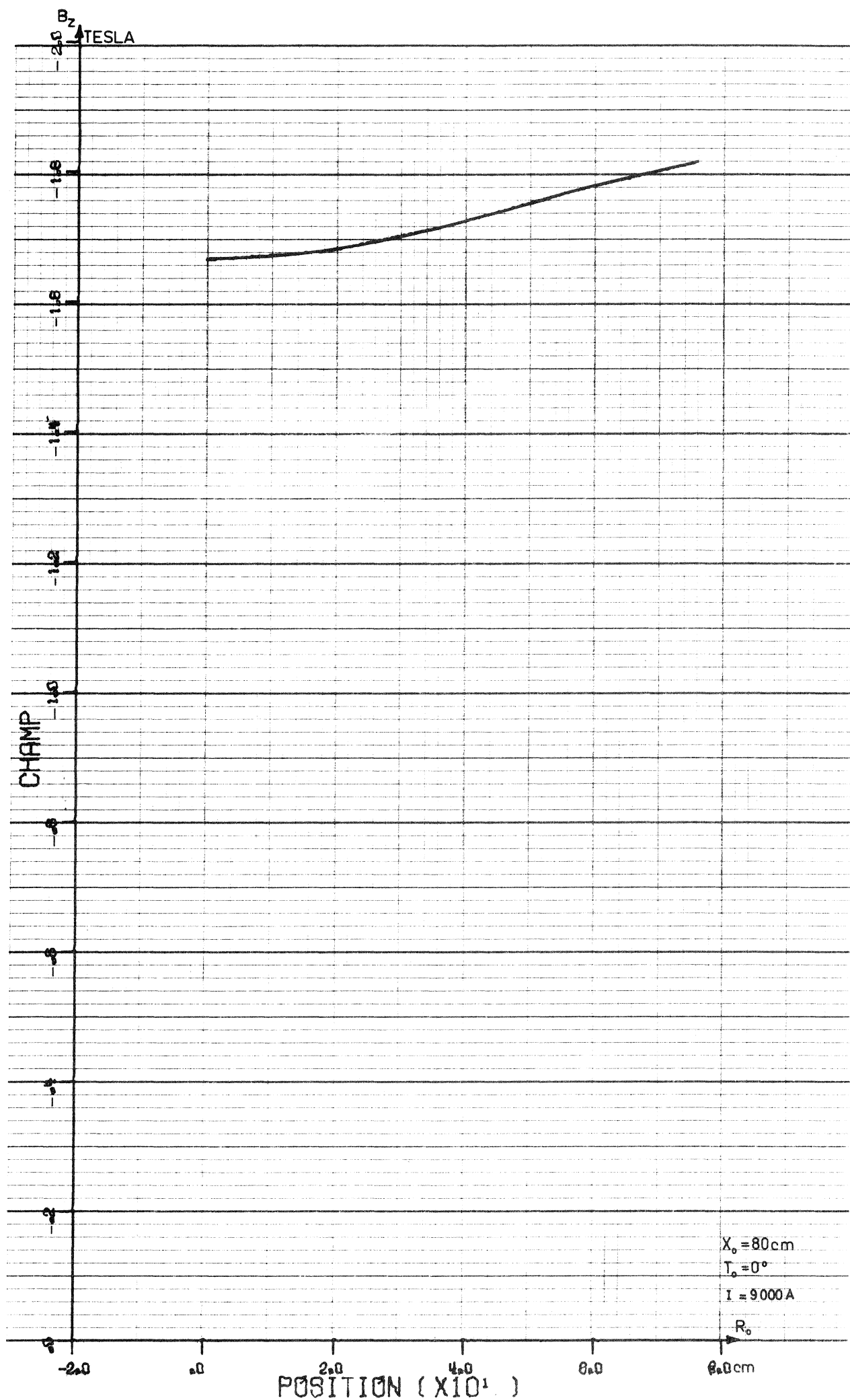


FIG.16

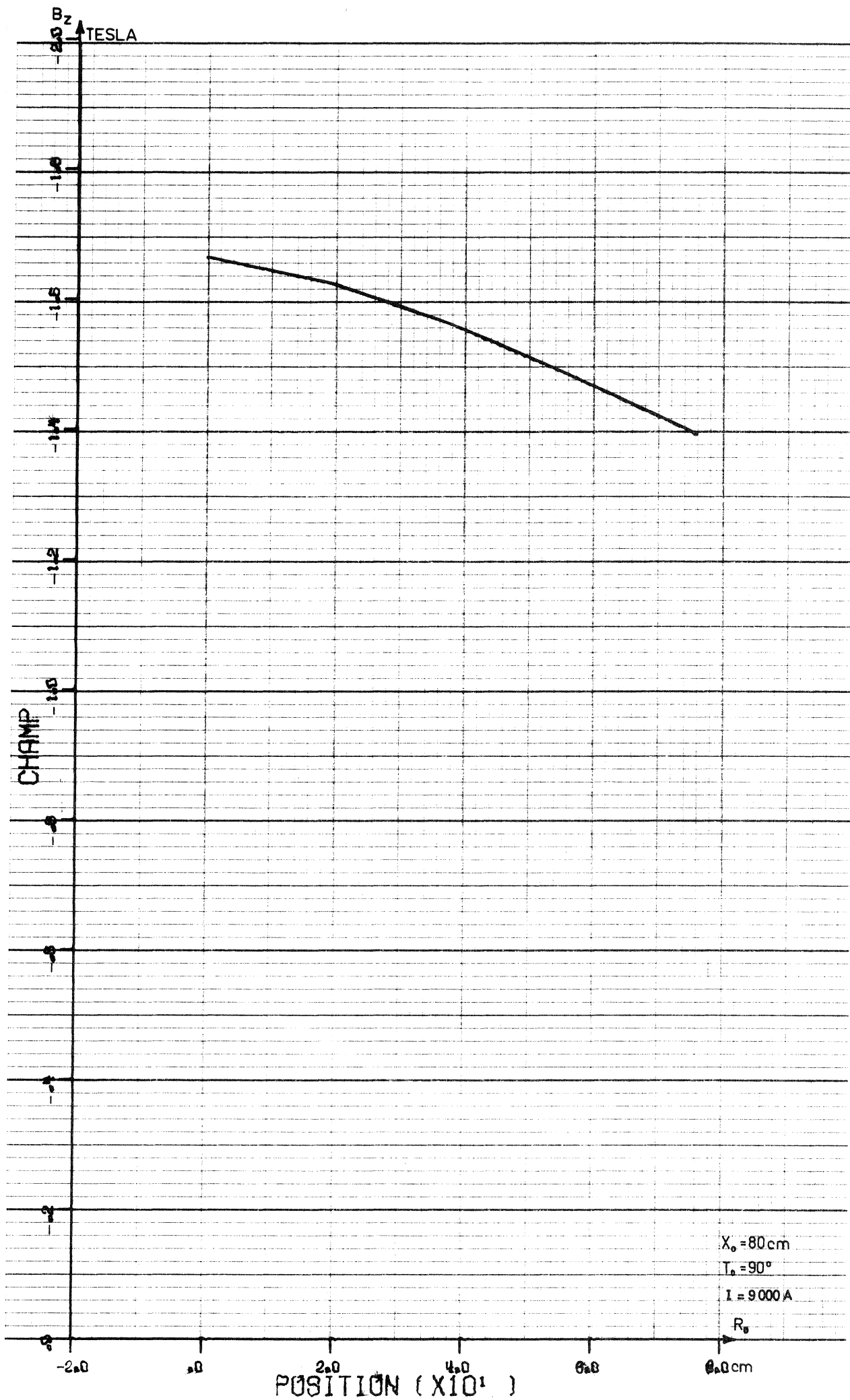


FIG. 17

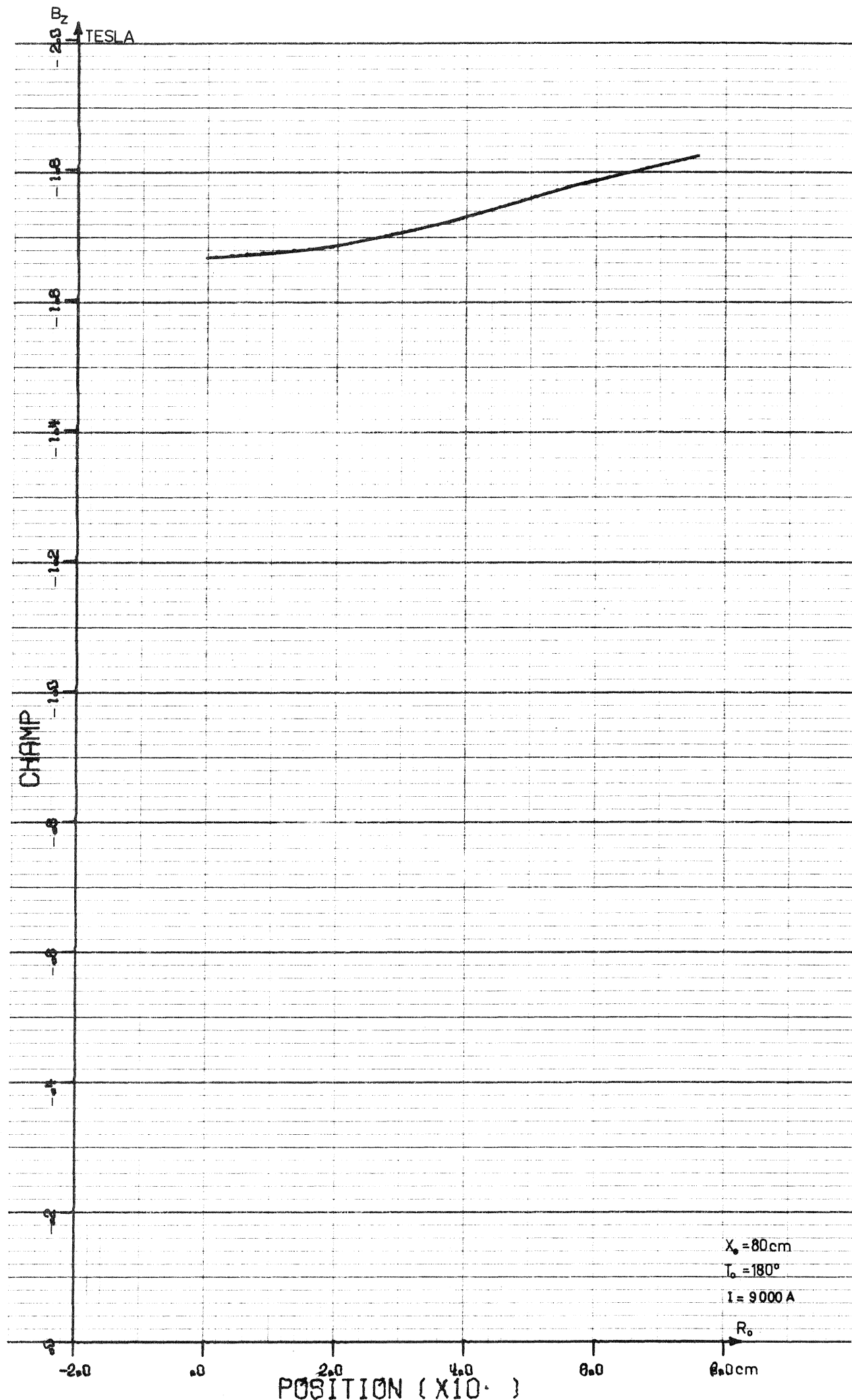


FIG. 18

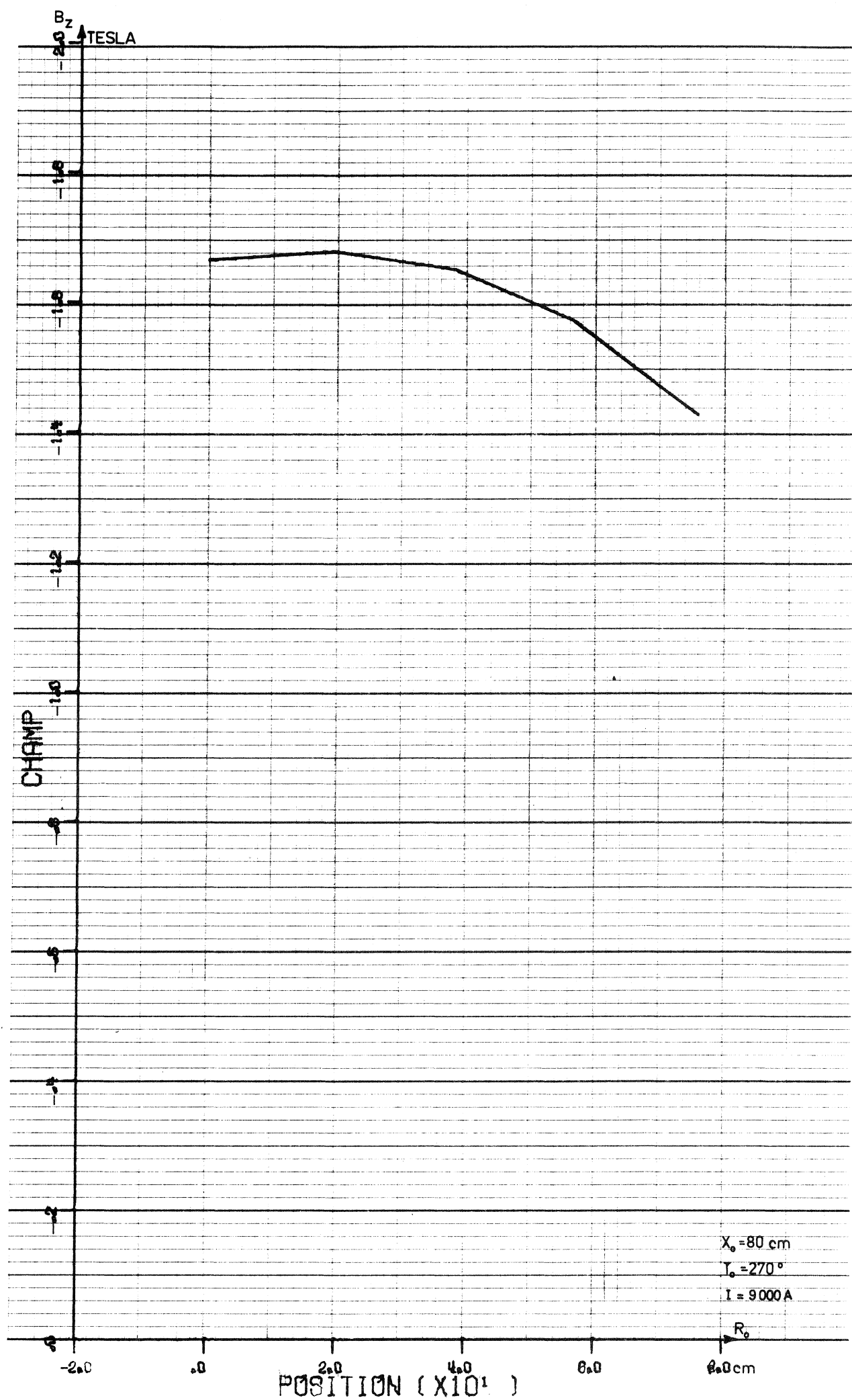


FIG.19

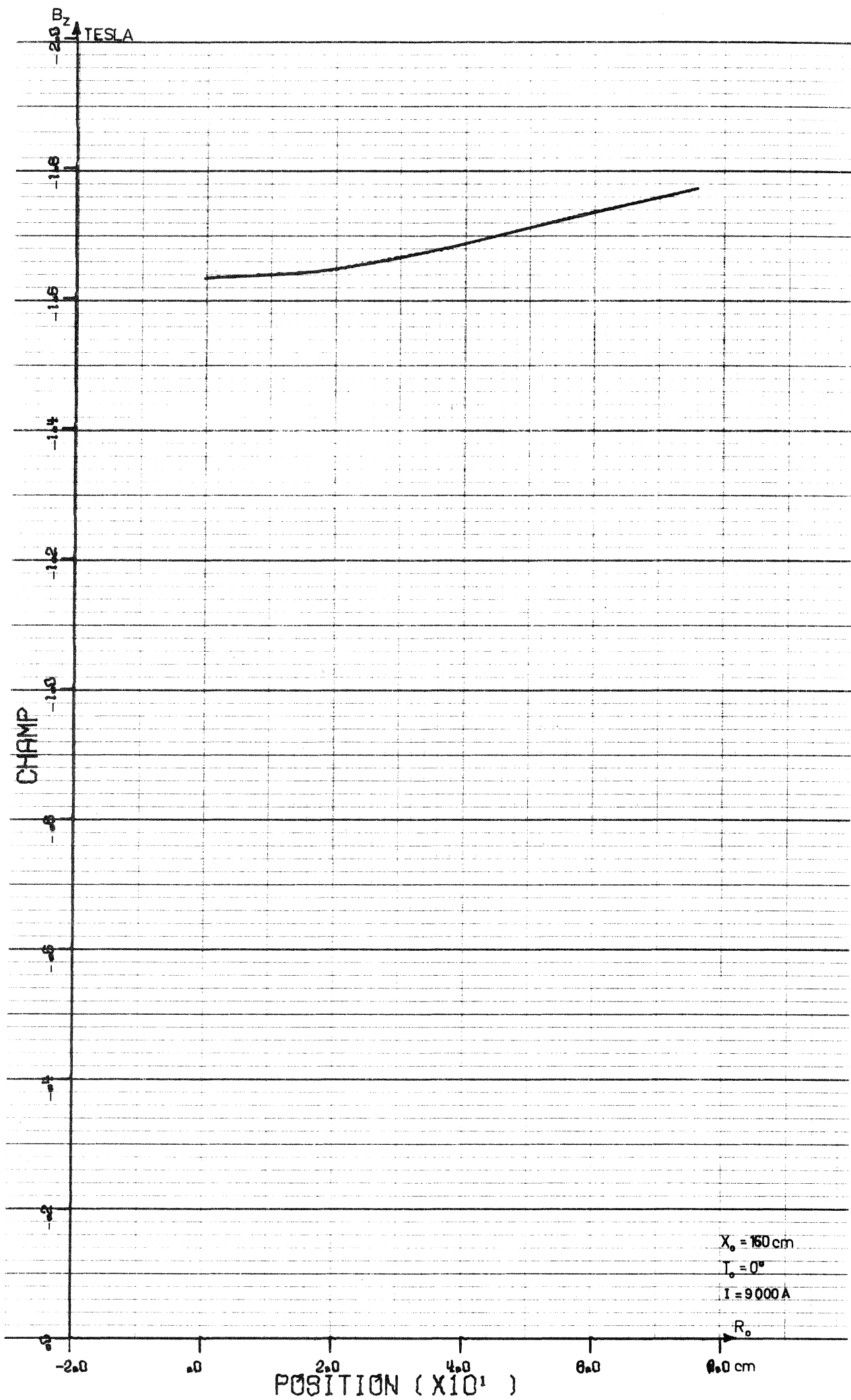


FIG. 20

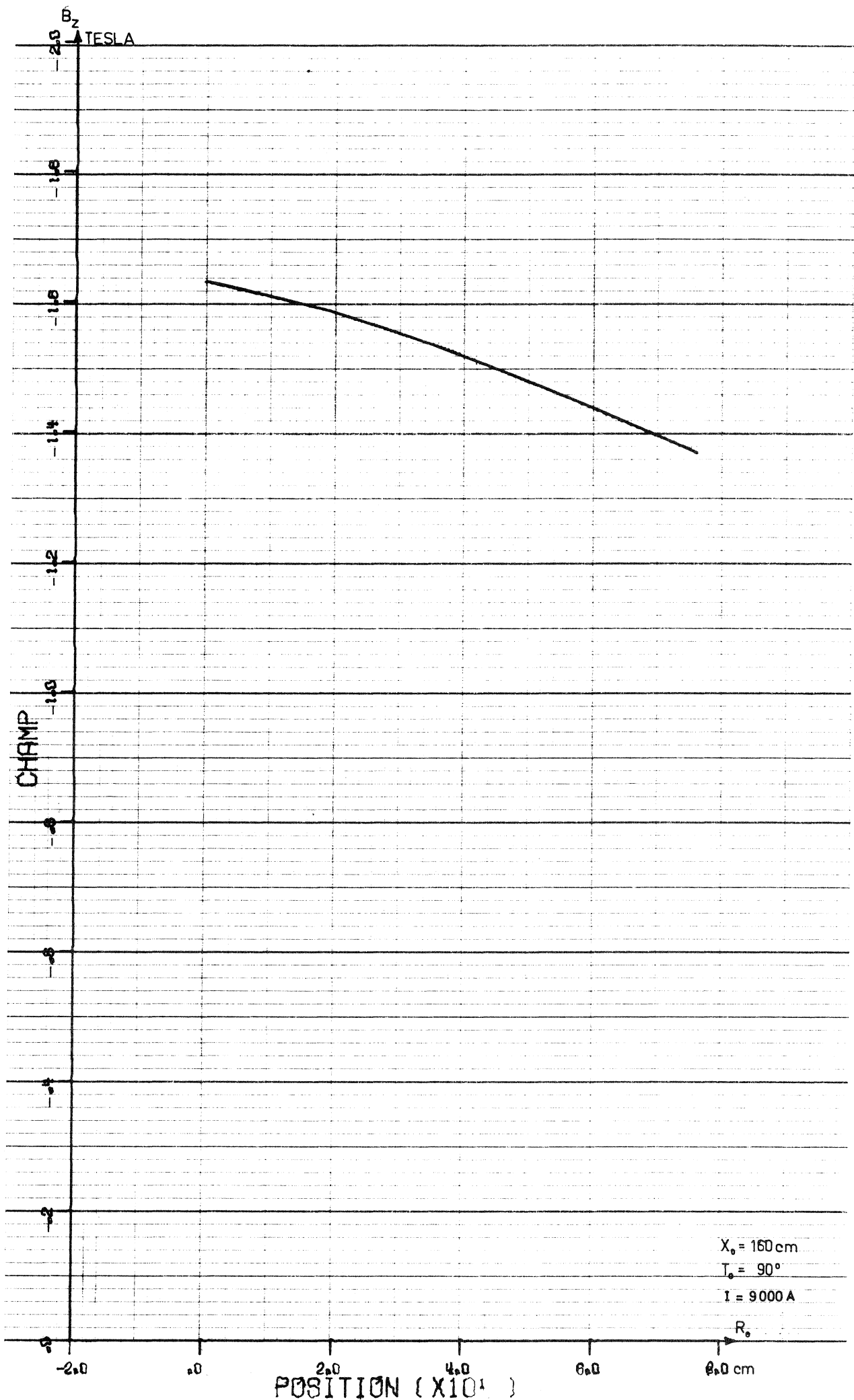


FIG. 21

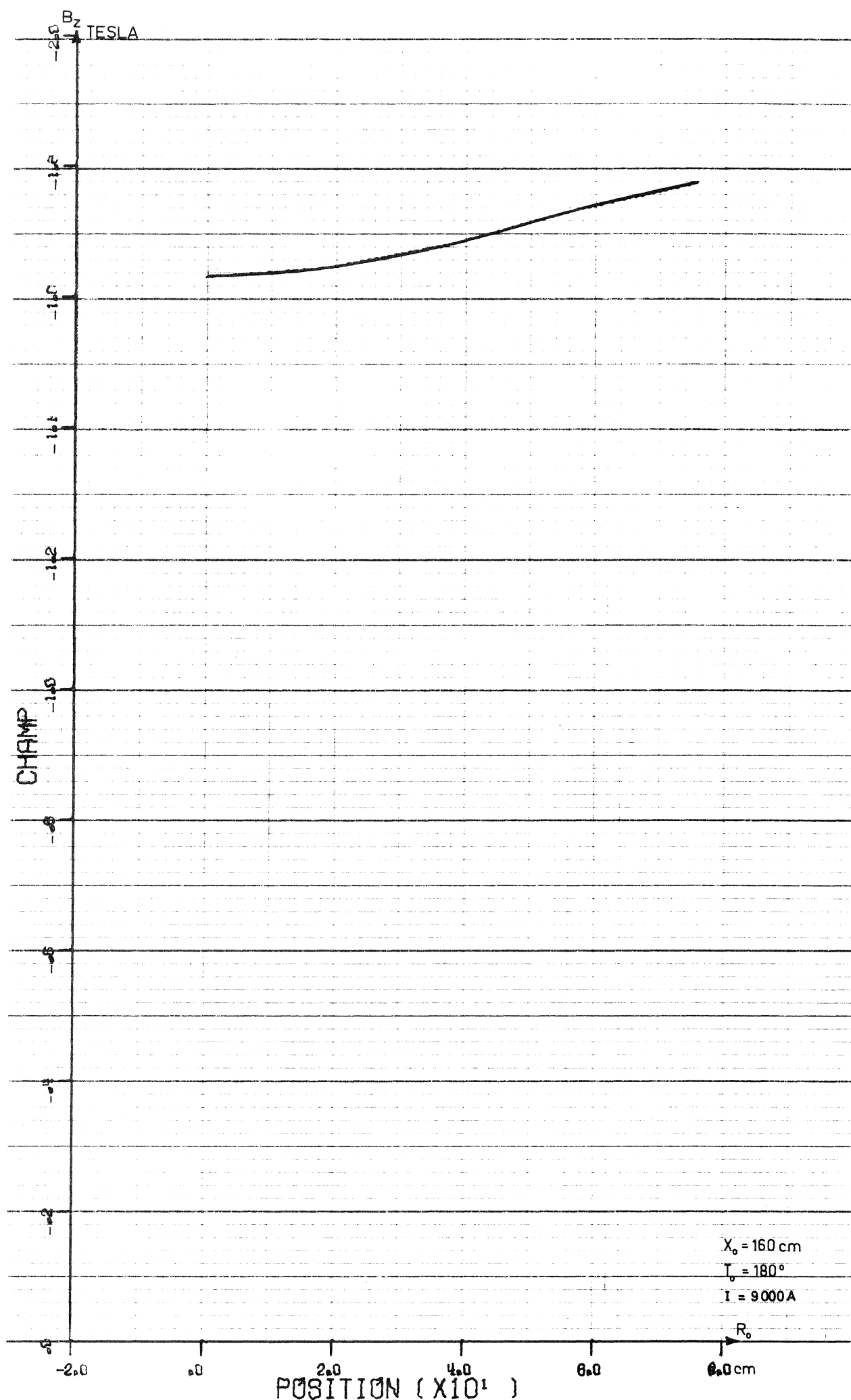


FIG. 22

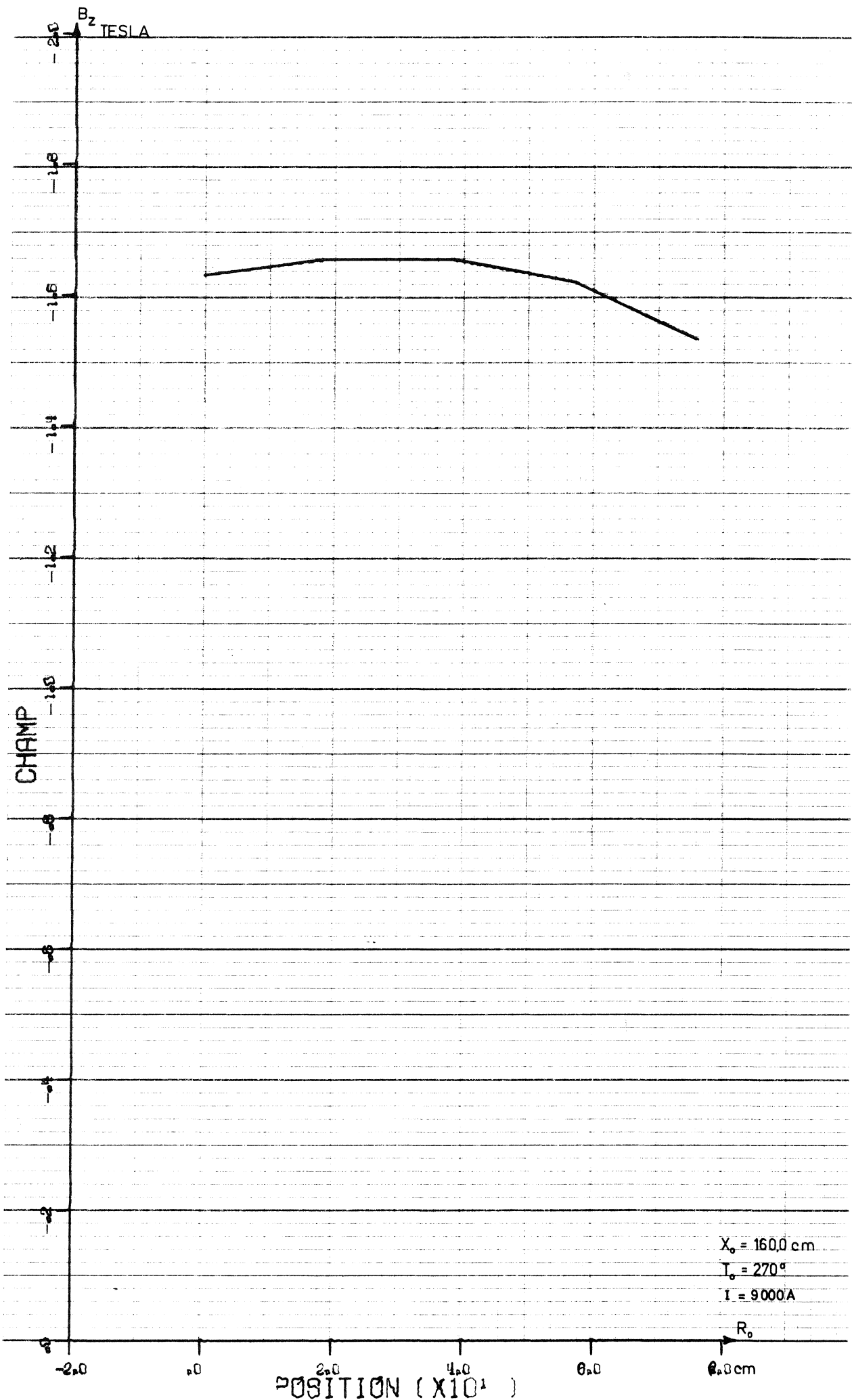


FIG. 23